Cell Reports

Article

TLR8 is activated by 5′-methylthioinosine, a *Plasmodium falciparum*-derived intermediate of the purine salvage pathway

Graphical abstract

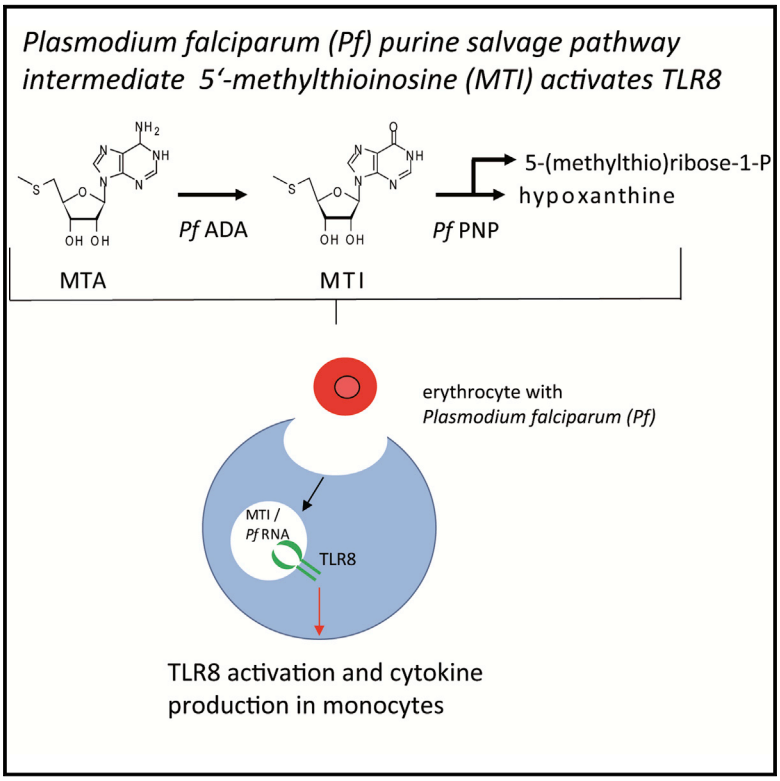

Highlights

- *Plasmodium falciparum*-derived 5′-methylthioinosine (MTI) activates Toll-like receptor 8
- Co-incubation with GU-rich RNA increases MTI stimulatory activity
- *Plasmodium falciparum*-derived MTI synergizes with RNA to stimulate human immune cells
- *Plasmodium falciparum*-infected erythrocytes induce IL-6 in an MTI- and TLR8-dependent manner

Authors

Gabriele Köllisch, Francisco Venegas Solis, Hannah-Lena Obermann, ..., Stefan Baumeister, Klaus Lingelbach, Stefan Bauer

Correspondence

stefan.bauer@staff.uni-marburg.de

In brief

Köllisch et al. identify 5′-methylthioinosine (MTI), a *Plasmodium*-derived metabolite of the purine salvage pathway, as Toll-like receptor 8 (TLR8) ligand. *In vitro* infection experiments with human PBMC and *P. falciparum*-infected red blood cells suggest that MTI serves as TLR8-dependent pathogen-associated molecular pattern (PAMP) for innate immune sensing.

Köllisch et al., 2022, Cell Reports *39*, 110691
April 12, 2022
https://doi.org/10.1016/j.celrep.2022.110691

CellPress

Cell Reports

CellPress
OPEN ACCESS

Article

TLR8 is activated by 5′-methylthioinosine, a *Plasmodium falciparum*-derived intermediate of the purine salvage pathway

Gabriele Köllisch,[1,8] Francisco Venegas Solis,[2] Hannah-Lena Obermann,[2] Jeannine Eckert,[1] Thomas Müller,[3] Tim Vierbuchen,[4] Thomas Rickmeyer,[5] Simon Muche,[6] Jude M. Przyborski,[7] Holger Heine,[4] Andreas Kaufmann,[2] Stefan Baumeister,[1] Klaus Lingelbach,[1,9] and Stefan Bauer[2,10,*]

[1]Department of Parasitology, Philipps University Marburg, 35043 Marburg, Germany
[2]Institute for Immunology, Philipps University Marburg, BMFZ, 35043 Marburg, Germany
[3]Institute for Medical Microbiology, Immunology und Hygiene, Technical University Munich, Munich, Germany
[4]Division of Innate Immunity, Research Center Borstel, Airway Research Center North (ARCN), German Center for Lung Research (DZL), Borstel, Germany
[5]Institute for Pharmaceutical Chemistry, Philipps University Marburg, 35043 Marburg, Germany
[6]Department of Chemistry, Philipps University Marburg, 35043 Marburg, Germany
[7]Department of Biochemistry and Molecular Biology, Interdisciplinary Research Center, Justus Liebig University Giessen, Giessen, Germany
[8]Present address: Research and Clinical Bioanalytics, CSL Behring Innovation GmbH, 35041 Marburg, Germany
[9]Deceased
[10]Lead contact
*Correspondence: stefan.bauer@staff.uni-marburg.de
https://doi.org/10.1016/j.celrep.2022.110691

SUMMARY

The innate immune recognition of the malaria-causing pathogen *Plasmodium falciparum* (*P. falciparum*) is not fully explored. Here, we identify the nucleoside 5′-methylthioinosine (MTI), a *Plasmodium*-specific intermediate of the purine salvage pathway, as a pathogen-derived Toll-like receptor 8 (TLR8) agonist. Co-incubation of MTI with the TLR8 enhancer poly(dT) as well as synthetic or *P. falciparum*-derived RNA strongly increase its stimulatory activity. Of note, MTI generated from methylthioadenosine (MTA) by *P. falciparum* lysates activates TLR8 when MTI metabolism is inhibited by immucillin targeting the purine nucleoside phosphorylase (PfPNP). Importantly, *P. falciparum*-infected red blood cells incubated with MTI or cultivated with MTA and immucillin lead to TLR8-dependent interleukin-6 (IL-6) production in human monocytes. Our data demonstrate that the nucleoside MTI is a natural human TLR8 ligand with possible *in vivo* relevance for innate sensing of *P. falciparum*.

INTRODUCTION

Malaria is caused by four species of Plasmodium: *P. vivax*, *P. ovale*, *P. malariae*, and *P. falciparum*, with *P. falciparum* causing the severe *malaria tropica* with high mortality. With 228 million cases of malaria and estimated 627,000 deaths worldwide in 2020 (World Health Organization, World malaria report, 2021), malaria poses a serious health problem.

In the past, significant research has increased our understanding of acquired immunity in malaria; however, the innate immune response to Plasmodium has not been studied extensively. In general, the innate immune system senses different classes of pathogen-associated molecular patterns (PAMPs) via germline-encoded pattern recognition receptors (PRRs), leading to immune activation and cytokine production (Takeuchi and Akira, 2010). Since this activation is a prerequisite for the initiation of the adaptive immune response, more insight in Plasmodium-derived structures that activate the innate immune system is desirable (Kalantari, 2018). Different classes of PRR, such as Toll-like receptors, C-type lectins, nucleotide-binding oligomerization domain (NOD)-like receptors (consisting of NOD and NLRP proteins), AIM2, cGAS, and RIG-I-like helicases, sense microbial structures on the cell surface, in the endosome and lysosome, or in the cytoplasm, respectively (Brubaker et al., 2015; Dolasia et al., 2018). Some of these sensors, such as NOD-like receptors and AIM2, can initiate the formation of the inflammasome, a cytosolic multiprotein complex that is required for processing of pro-interleukin-1β (IL-1β) and consists of the sensor, the adaptor protein apoptosis associated speck-like protein containing a CARD (ASC), and the effector caspase-1 (Bauernfeind and Hornung, 2013).

Plasmodium-derived PAMPs are the heme detoxification product hemozoin and glycosylphosphatidylinositol (GPI) anchors that trigger the NLRP3/NLRP12 inflammasome (Ataide et al., 2014) and TLR2–TLR1 heterodimer (Zhu et al., 2011), respectively. Innate recognition of Plasmodium DNA is mediated by nucleic acid sensors, such as TLR9, cGAS (Sharma et al., 2011; Sisquella et al., 2017; Gallego-Marin et al., 2018; Hahn

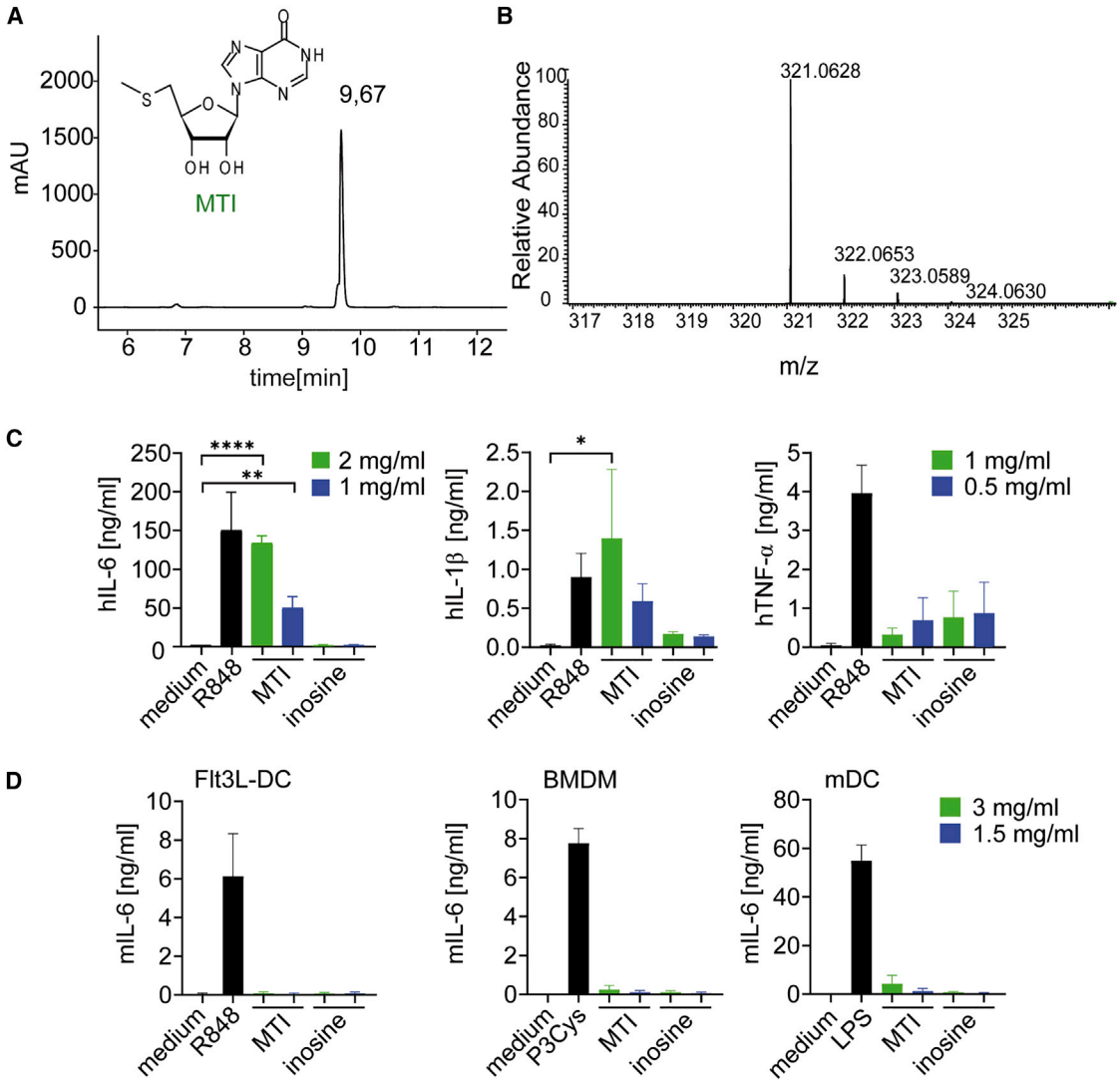

Figure 1. MTI activates human, but not murine immune cells

(A) MTI was purified via RP-HPLC, and corresponding UV detection is depicted.

(B) Mass spectrometry analysis of MTI.

(C) hPBMCs were stimulated with the TLR ligand R848 as positive control as well as MTI and inosine at 2 mg/mL, 1 mg/mL, or 0.5 mg/mL. After 24 h of incubation, the supernatants were analyzed for IL-6 (biological replicates: 3; technical replicates: 1–3), IL-1β (biological replicates: 4; technical replicates: 2–3), and TNF-α (biological replicates: 2; technical replicates: 3) by ELISA.

(D) Primary mouse bone marrow cells were differentiated with FLT3 ligand, macrophage colony stimulating factor (M-CSF), or granulocyte-macrophage colony-stimulating factor (GM-CSF) to Flt3L-DC (biological replicates: 3; technical replicates: 3); BMDM (biological replicates: 2; technical replicates: 2–3); or mDC (biological replicates: 2; technical replicates 2–3), respectively and stimulated with control stimuli (R848, P3Cys, and LPS) as well as MTI and inosine at 3 mg/mL and 1.5 mg/mL. IL-6 levels were quantified by ELISA.

(C and D) Bars indicate mean + SEM. Statistical significance was determined by one-way ANOVA with Dunnett's post-hoc test. *$p < 0.05$, **$p < 0.01$, and ****$p < 0.0001$.

et al., 2018), and AIM2 (Kalantari et al., 2014). In addition, Plasmodium-derived RNA is recognized by TLR7 and TLR8 (Baccarella et al., 2013; Coch et al., 2019), which are single-stranded RNA sensors (Diebold et al., 2004; Heil et al., 2004; Lund et al., 2004).

In general, activation of TLR7 is mediated by guanosine- and uridine-rich single-stranded RNA (ssRNA) or polyuridine (Diebold et al., 2004; Heil et al., 2004). Guanosine- and uridine-rich ssRNA also activates TLR8, but adenosine can replace guanosine without affecting the immunostimulatory potential (Heil et al., 2004; Forsbach et al., 2008; Krüger et al., 2015). Structural analysis further provided insight into RNA receptor interaction by demonstrating that actually degradation products, such as nucleosides and oligoribonucleotides, bind to TLR7 and TLR8

Table 1. LPS content of the MTI and inosine preparation

Substance	LPS (pg/mL)
MTI	0
Inosine	0
LPL (Burkholderia sp.)	>2,000
LPS (as positive control) 50 pg/mL	41.9

The amount of LPS was quantified with the limulus amebocyte lysate (LAL) test for MTI, inosine (3 mg/mL), and lipoprotein lipase (LPL) from Burkholderia sp. (250 μg/mL) and LPS (50 pg/mL). Commercially available LPL from gram− bacteria served as an additional positive control since it is usually heavily contaminated with LPS.

(Tanji et al., 2015; Zhang et al., 2016, 2018b). Recently, the RNase T2 and RNase 2 have been identified as essential RNases for the generation of oligoribonucleotides and uridine from bacterial, plasmodial, or synthetic RNAs to activate TLR8 (Greulich et al., 2019; Ostendorf et al., 2020).

For activation of TLR7 and TLR8, two distinct binding sites have to be occupied: nucleosides (guanosine for TLR7 and uridine for TLR8) bind to the conserved site 1, whereas oligoribonucleotides interact with site 2. Since site 2 is not as conserved, different sequence requirements for oligoribonucleotide binding to TLR7 and TLR8 are observed. In general, interaction with site 2 enhances binding affinities of site 1 and supports receptor dimerization. Guanosine, guanosine analogs (Heil et al., 2003, 2004; Lee et al., 2003; Shibata et al., 2016), and imidazoquinolines (e.g., imiquimod or resiquimod) have been described to activate TLR7 and/or TLR8 (Hemmi et al., 2002; Jurk et al., 2002). This activation is mediated by interaction with site 1 and subsequent receptor dimerization (Tanji et al., 2013; Zhang et al., 2018b). TLR8 activation can also be strongly enhanced by T-rich phosphorothioate oligodeoxynucleotides (Jurk et al., 2006); however, the mechanism is currently unknown. In addition, inosine incorporation into RNA mediated by ADAR1 editing can also modulate TLR7 and TLR8 activation (Sarvestani et al., 2014).

TLR7 and TLR8 dimerization leads to recruitment of the adaptor protein myeloid differentiation primary response 88 (MyD88), culminating in activation of different kinases and transcription factors nuclear factor κB (NF-κB) and/or IRF5 and IRF7, leading to proinflammatory cytokine and/or type I interferon production (O'Neill, 2006). The signaling cascade triggered by TLR8 differs in some respect to TLR7, since only TLR8 can activate the NLRP3 inflammasome and induce IL-1β production in human monocytes (Vierbuchen et al., 2017).

In the quest for new Plasmodium-derived PAMPs, we focused on purine metabolisms. In contrast to the human host, *Plasmodium falciparum* lacks *de novo* purine synthesis, and therefore, purines formed as products of polyamine synthesis are recycled in a novel pathway in which 5′-methylthioinosine (MTI) is generated by *P. falciparum* adenosine deaminase (*Pf*ADA) and converted to hypoxanthine by *P. falciparum* purine nucleoside phosphorylase (*Pf*PNP) (Ting et al., 2005). The conversion of 5′-methylthioadenosine (MTA) to MTI has also been reported for other Plasmodium species (e.g., *P. vivax* and *P. berghei*; Ho et al., 2009). Immucillins, such as 5′-methylthio-immucillin-H, are specific *Pf*ADA inhibitors that lead to parasite death and therefore may have clinical potential as anti-malarials (Evans et al., 2018).

Here, we demonstrate that MTI is a naturally occurring purine that activates human immune cells. Using genetic reconstitution, CRISPR-Cas9 knockout cells, the TLR8 inhibitor CU-CPT9a (Hu et al., 2018; Zhang et al., 2018b), and molecular modeling, we demonstrate that MTI is a TLR8-specific agonist presumably binding to site 1 of TLR8. The activity of MTI can be enhanced by low concentrations of Plasmodium-derived RNA, synthetic ssRNA, or poly(dT). Furthermore, inhibition of *Pf*PNP by immucillins leads to accumulation of MTI, driving immune activation of Plasmodium-infected monocytes, suggesting that use of immucillins may boost TLR8-mediated immunity against Plasmodium.

RESULTS

MTI activates human PBMC

For the analysis of immunostimulation by pathogen-specific nucleosides, we selected the purine MTI as a suitable candidate. MTI is part of the purine salvage pathway in *Plasmodium ssp.* (Ting et al., 2005) and few bacterial species, such as *Pseudomonas aeruginosa* (Guan et al., 2011) and *Methanocaldococcus jannaschii* (Miller et al., 2018). As MTI is commercially not available, we generated this nucleoside by deaminating MTA using $NaNO_2$ (Kotra et al., 1996). MTI was purified by reversed-phase high-performance liquid chromatography (RP-HPLC) and the identity confirmed by mass spectrometry (Figures 1A and 1B). Inosine was generated with the identical procedure by deamination of adenosine and served as negative control in stimulation experiments. When human peripheral blood mononuclear cells (PBMCs) were incubated with MTI or inosine at 2, 1, and 0.5 mg/mL, only MTI induced cytokines, such as IL-6 and IL-1β (Figure 1C). In contrast, the proinflammatory cytokine tumor necrosis factor alpha (TNF-α) was not induced (Figure 1C). Of note, murine plasmacytoid dendritic cells (Flt3L-DCs), murine bone-marrow-derived macrophages (BMDMs), and myeloid dendritic cells (mDCs) (Figure 1D) did not respond to MTI stimulation with IL-6 production, indicating murine immune cells as being non-responsive to MTI.

To exclude that the stimulating effect of MTI is due to possible contamination with TLR4 ligands, the lipopolysaccharide (LPS) content of MTI was tested by the Limulus assay and found to be below the detection limit of the assay (Table 1).

MTI is recognized in a TLR8-dependent manner

Utilizing genetic complementation assays, stimulation of TLR-deficient cells, and inhibitory studies, we investigated whether nucleic-acid-sensing TLRs were involved in MTI-driven immune activation. Of note, TLR8 (and NF-κB reporter)-transfected HEK-293 cells were activated by MTI, whereas TLR7-transfected cells did not respond to this stimulus (Figure 2A). Inosine served as negative control and activated neither TLR7 nor TLR8. However, TLR7- and TLR8-transfected cells were stimulated by the positive control resiquimod (R848; Figure 2A). MTA was not used as an additional specificity control, as MTA is toxic to cells (Riscoe et al., 1984; Lee and Cho, 1998). The MTI concentrations used resemble immunostimulatory concentrations observed for other stimulatory nucleosides, such as loxoribine (Heil et al., 2003;

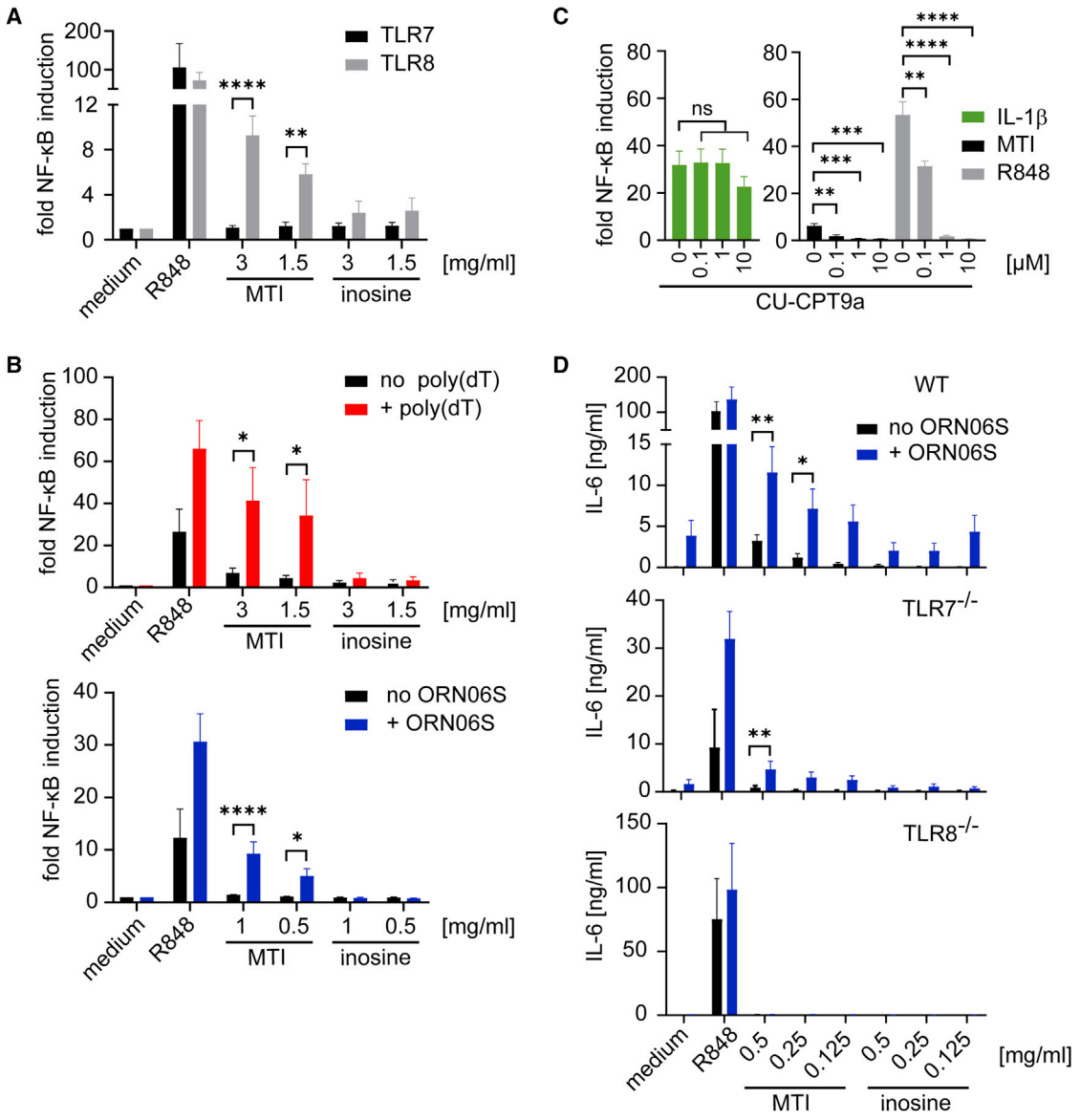

Figure 2. MTI activation is TLR8-dependent

(A) HEK-293 hTLR8^{+}Nf^{+} or hTLR7^{+}Nf^{+} transfected cells were incubated with medium, R848, MTI, and inosine (3 mg/mL and 1.5 mg/mL). Cells were lysed after 24 h of incubation, and luciferase activity was determined (biological replicates: 3; technical replicates: 2–3).

(B) Stimulation of HEK-293 TLR8^{+}Nf^{+} cells was performed by co-incubation of MTI and inosine (3 mg/mL and 1.5 mg/mL) with or without 3 μM of poly(dT) or 150–300 ng/mL ORN06S. After 24 h of stimulation, cells were lysed and the luciferase activity was measured (biological replicates: 3; technical replicates for poly(dT) co-stimulation and biological replicates: 4; technical replicates: 3 for ORN06S co-stimulation).

(C) HEK-blue hTLR8 cells were incubated with different concentrations of CU-CPT9a as indicated and 0.5 mg/mL MTI or 1 μM R848 or 10 ng/mL IL-1β and 1 μM poly(dT) (biological replicates: 3; technical replicates: 3).

(D) BLaER1 WT, TLR7$^{-/-}$, and TLR8$^{-/-}$ cells were stimulated with R848, MTI, and inosine (0.5 mg/mL, 0.25 mg/mL, and 0.125 mg/mL) in co-incubation with 50 ng/mL ORN06S. hIL-6 was measured by ELISA (biological replicates: 4; technical replicates: 3).

Bars indicate mean + SEM. Statistical significance was determined by two-way ANOVA with Sidak's post-hoc test (A, B, and D) or one-way ANOVA with Dunnett's post-hoc test (C). *p < 0.05, **p < 0.01, ***p < 0.001, and ****p < 0.0001. ns, not significant.

Lee et al., 2003) but are presumably non-physiological. Therefore, we investigated whether co-administration of the TLR8-co-activator poly(dT) (Jurk et al., 2006) or synthetic RNA, such as the phosphorothioate-modified ORN06S (Forsbach et al., 2008; Tanji et al., 2015), augments the response to lower MTI concentrations. Of note, TLR8-transfected HEK-293 cells demonstrated strongly enhanced induction of TLR8-mediated NF-κB activation when stimulated with MTI and poly(dT) (Figure 2B).

Similarly, the synthetic oligoribonucleotide ORN06S led to increased MTI-mediated TLR8 activation when co-transfected

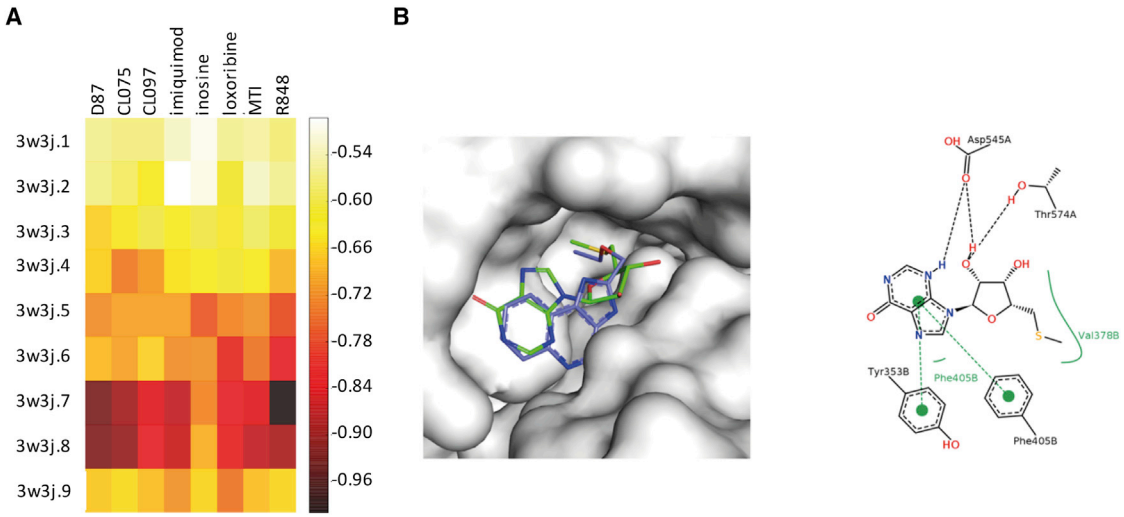

Figure 3. Modeling of MTI-TLR8 interaction

(A) Visualization of the docking scores for the best ranked docking poses of each ligand in each of the putative binding pockets of TLR8 (PDB: 3W3J). Deep red indicates favorable interactions.

(B) The binding mode of 5′-methylthioinosine and possible interactions with TLR8 predicted by GOLD.

with the cationic lipid reagent DOTAP or pLA (Figure 2B). To obtain further evidence that MTI activates TLR8, we stimulated TLR8-expressing HEK-293 cells with MTI and poly(dT) and increasing concentrations of the TLR8 antagonist CU-CPT9a (Hu et al., 2018; Zhang et al., 2018b). Supporting the notion of a TLR8-specific agonist, MTI-driven activation was inhibited by CU-CPT9a in a dose-dependent manner similar to the inhibition of R848 activity (Figure 2C). In contrast, IL-1β-driven NF-κB activation of HEK-293 cells was not influenced by the antagonist (Figure 2C).

We further explored the TLR8-dependent activity of MTI in human immortalized immune cells and utilized wild-type (WT) as well as TLR7- or TLR8-deficient BLaER1 cells differentiated to macrophages (Guan et al., 2011; Vierbuchen et al., 2017; Gaidt et al., 2018). Stimulation with MTI and the TLR8 enhancer ORN06S revealed that WT and TLR7-deficient macrophages responded with IL-6 production, whereas TLR8-deficient cells were not activated (Figure 2D). Inosine showed no activity in general with or without RNA co-stimulation. In summary, MTI specifically activates TLR8 and activity can be strongly enhanced by poly(dT) or single-stranded GU-rich RNA.

3D modeling and docking analysis with programs GOLD and FlexX further supported the direct interaction of MTI with TLR8. Assuming that MTI binds site 1, the same binding pocket as the other agonists (e.g., RX8, C09, L07, and D87; Tanji et al., 2013), and since GOLD was able to reproduce correctly the binding mode of the known ligand C09 (data not shown), we assume that GOLD predicted a reasonable docking solution for MTI (Figure 3A, Table 2). MTI (shown in green) adopts a similar binding mode as C09 (shown in blue) in its crystal structure. The hypoxanthine moiety is able to form pi-pi interactions to Tyr353 and Phe405. The ribofuranose is involved in polar interactions. Furthermore, the hydrophobic part at the bottom of the pocket is addressed, which appears to be crucial for agonistic activity (Figure 3B).

Table 2. Volume and the hosted ligand of the cavities of TLR8 detected by LIGSITE

Cavity ID	Volume [Å^3]	Ligand
3w3j.1	300.5	-
3w3j.2	397.5	-
3w3j.3	395.0	-
3w3j.4	477.1	-
3w3j.5	505.8	-
3w3j.6	534.4	-
3w3j.7	621.6	C09
3w3j.8	689.6	C09
3w3j.9	1172.0	-

Plasmodium falciparum-derived MTI synergizes with RNA to stimulate human immune cells

To analyze the immunostimulatory role of MTI in a more physiological setting, we investigated whether *P. falciparum* lysates would support MTI synthesis. Of note, in *P. falciparum*, MTA is converted to MTI by *Pf*ADA and further metabolized to hypoxanthine by *Pf*PNP releasing 5-(methylthio)ribose-1-P (Figure 4A). Enzymatic function of *Pf*ADA and *Pf*PNP can be inhibited by pentostatin (2′-deoxycoformycin; Webster et al., 1984) and immucillins (Evans et al., 2018), respectively. Interestingly, when MTA was added to *Pf* lysates and *Pf*PNP was inhibited by the addition of DADMe-immucillin-H, MTI accumulated in the lysates as detected by HPLC analysis (Figure 4B). In contrast, pentostatin-treated lysates did not produce any MTI as *Pf*ADA was inhibited (Figure 4B).

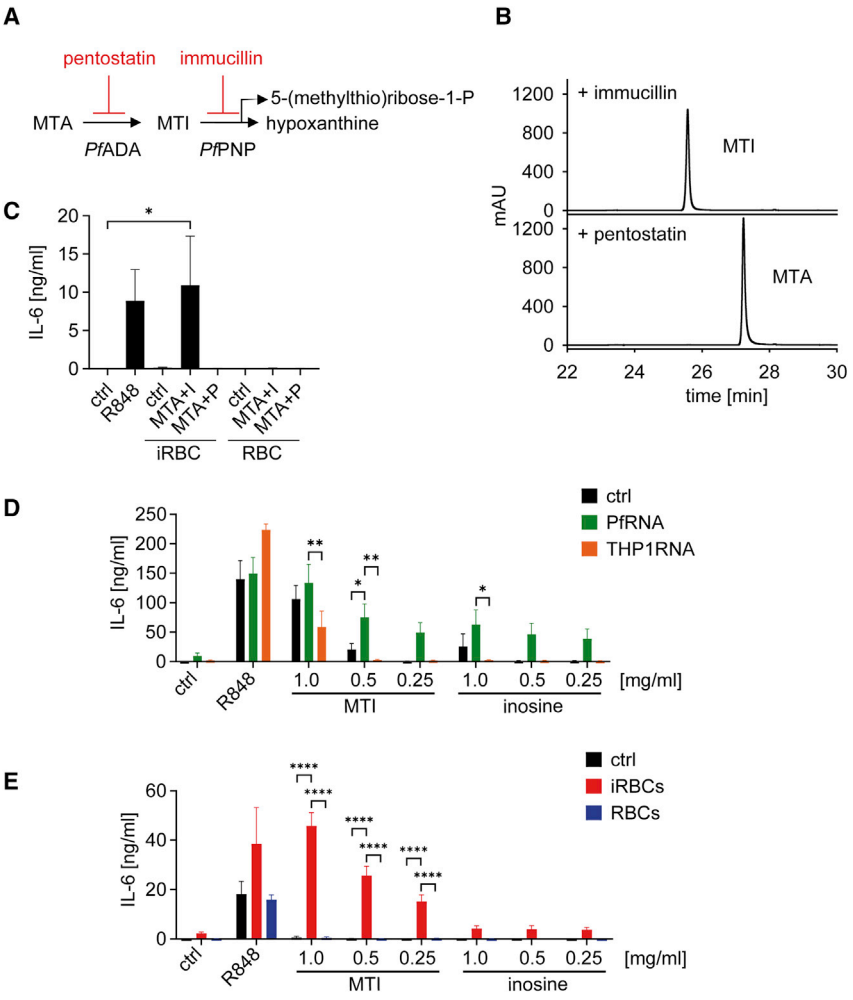

Figure 4. *Plasmodium falciparum*-derived MTI synergizes with RNA to stimulate human immune cells

(A) Pathway description of MTA conversion to MTI and hypoxanthine with corresponding enzymes and inhibitors.

(B) Lysates from iRBCs and RBCs were incubated with MTA and immucillin (10 μM) or pentostatin (10 μM), and the conversion to MTI was monitored by RP-HPLC.

(C) hPBMCs were incubated with iRBC lysate or RBC lysate, ctrl (medium only), MTA + I (MTA 1 mg/mL; immucillin), and MTA + P (MTA 1 mg/mL; pentostatin). Twenty-four hours after stimulation, hIL-6 in the supernatant was quantified by ELISA (biological replicates: 3; technical replicates: 2–3).

(D) Human monocytes were stimulated with control stimuli, MTI, or inosine (1.0 mg/mL, 0.5 mg/mL, and 0.25 mg/mL) without RNA (ctrl) and each in co-incubation with 150 ng/mL RNA from *Plasmodium falciparum* (PfRNA) or THP-1-derived RNA (THP1RNA). IL-6 was analyzed by ELISA (biological replicates: 4; technical replicates: 2–3).

(E) hPBMCs were stimulated with R848, MTI, or inosine without RBCs (ctrl) or co-incubated with opsonized iRBCs or RBCs. After 24 h of incubation, the supernatant was analyzed for hIL-6 by ELISA (biological replicates: 2; technical replicates: 2–3).

(C–E) Bars indicate mean + SEM. Statistical significance was determined by one-way ANOVA with Dunnett's post-hoc test (C) or two-way ANOVA with Tukey's post-hoc test (D and E). *$p < 0.05$, **$p < 0.01$, and ****$p < 0.0001$.

Subsequently, hPBMCs were incubated with lysates of either infected red blood cells (iRBCs) or non-infected RBCs that were untreated or incubated with MTA and DADMe-immucillin-H (MTA + I) or MTA and pentostatin (MTA + P) (Figure 4C). The iRBC lysate alone as well as the RBC lysate did not stimulate hPBMCs. If MTA was converted to MTI by the iRBC lysate and accumulated by use of DADMe-immucillin-H, immune stimulation was prominent. In contrast, pentostatin abolished this effect, as MTA was not converted to MTI. RBC lysates incubated with MTA and immucillin or pentostatin had no immunostimulatory effects (Figure 4C).

During *P. falciparum* infection, monocytes can phagocytose *P. falciparum*-infected RBCs and are immune activated (Gazzinelli et al., 2014). We hypothesized that MTI reaches the endosomal TLR8 via this route and *P. falciparum*-derived RNA may act as co-factor and TLR8 enhancer as described for poly(dT) or the synthetic ORN06S. To test this hypothesis, we co-incubated primary human monocytes or human PBMCs with MTI and either *Pf*RNA or *P. falciparum*-infected iRBCs, respectively (Figures 4D and 4E). The *Pf*RNA concentration used for stimulation was selected to be non- or weakly stimulative. Co-incubation of *Pf*RNA with MTI strongly increased IL-6 production at higher nucleoside concentrations in human monocytes (Figure 4D). In contrast, the same amount of THP-1-derived RNA did not increase MTI-driven cytokine production and even demonstrated some inhibitory effect (Figure 4D). For inosine stimulation, a small enhancement of IL-6 production with *Pf*RNA was detectable at high concentrations, although in general, the background of immune stimulation of *Pf*RNA in the context of either nucleoside was increased compared with RNA stimulation without nucleosides (Figure 4D). Similarly, in PBMCs, MTI stimulation and concurrent phagocytosis of *P. falciparum*-infected RBCs led to an IL-6 production in an MTI-concentration-dependent manner (Figure 4E). In contrast, uninfected RBCs did not enhance MTI-mediated immune stimulation (Figure 4E). These observations strengthen the hypothesis that MTI and *P. falciparum* RNA as cofactor mediate immune recognition of this parasite via TLR8 in human immune cells.

To demonstrate a more physiological role of endogenous MTI during *P. falciparum* innate immune sensing, we stimulated human PBMC with *P. falciparum*-infected RBCs or uninfected RBCs under conditions where MTI is produced and measured the induction of IL-6. With low hypoxanthine concentrations (Hx) (20 μM) as sole purine source, iRBCs only induced minor amounts of IL-6. Under this condition, the addition of immucillin had no modulating effect, suggesting that the levels of MTI were not sufficient to induce high levels of IL-6. However, when MTA

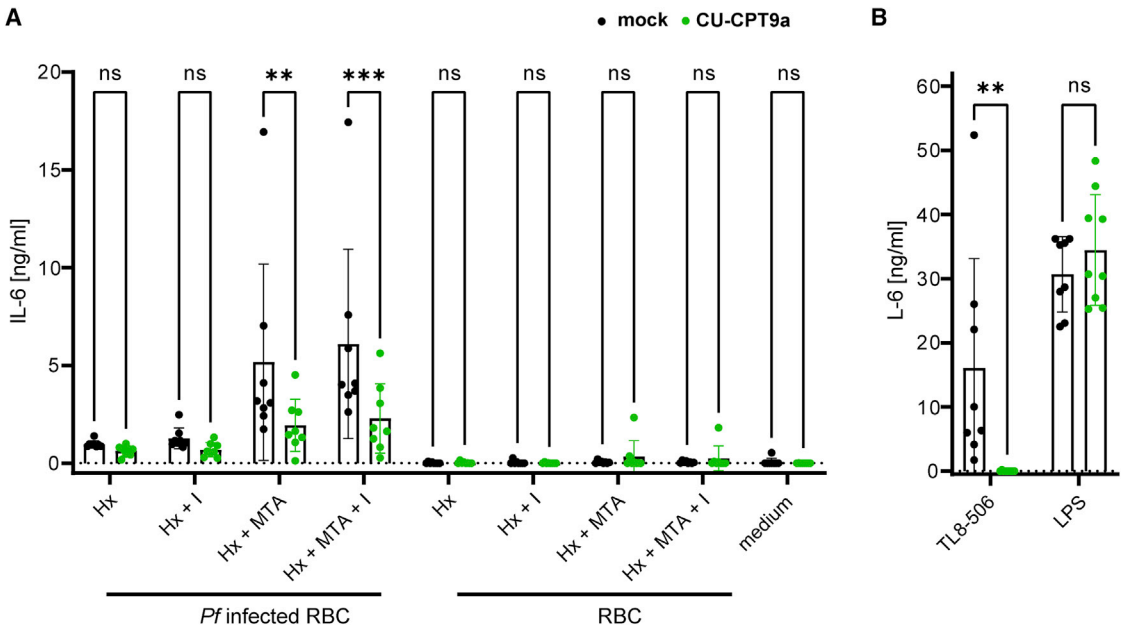

Figure 5. *Plasmodium falciparum*-produced MTI activates TLR8 during *in vitro* infection of PBMCs

PBMCs from eight different donors adjusted to 100,000 monocytes/well were incubated (A) with highly enriched *P. falciparum*-infected RBCs (>90% parasitemia) and non-infected RBCs at a multiplicity of infection (MOI) of 3 in relation to monocytes or (B) with TLR8 ligand TL8-506 (120 nM) or LPS (1 ng/mL). Cell culture was performed without (black dot) or with (green dot) the TLR8 inhibitor CU-CPT9a in RPMI-2% AB-serum and, for RBC/iRBC stimulation, contained additionally hypoxanthine (Hx), hypoxanthine (100 μM) plus immucillin (10 μM) (Hx + I), hypoxanthine (100 μM) plus MTA (100 μM) (Hx + MTA), or hypoxanthine (100 μM) plus MTA (100 μM) and immucillin (10 μM) (Hx + MTA + I) as indicated (biological replicates: 8; technical replicates: 2). Bars indicate mean + SEM. Statistical significance was determined with ANOVA followed by Bonferroni's multiple comparison test. **$p < 0.01$ and ***$p < 0.001$. ns, not significant.

was added as an additional purine source, iRBCs strongly induced IL-6. Importantly, the addition of the TLR8 inhibitor CU-CPT9a significantly reduced IL-6 production, supporting the notion that TLR8 is an important innate sensor for *P. falciparum* metabolites. The addition of immucillin had only minor effects in enhancing IL-6 production, which is probably because the threshold of TLR8-activating MTI concentrations was already reached without the addition of immucillin (Figure 5A). As specificity control, LPS-induced IL-6 production was not inhibited by the TLR8 inhibitor CU-CPT9a, whereas the stimulatory activity of TL8-506, a synthetic TLR8 ligand, was blunted (Figure 5B).

In further experiments, we analyzed the metabolic conversion of nucleosides in the purine salvage pathway of iRBCs and RBCs utilizing HPLC. Under control conditions with only hypoxanthine in the culture medium, iRBCs and RBCs produced no detectable MTI or MTA. However, when cells were incubated with MTA and/or immucillin for 1 h, striking differences were detectable in inosine, MTI, and MTA concentrations (Table 3). MTA is efficiently converted to MTI in the supernatant of iRBCs, whereas RBCs hardly metabolize MTA and generate MTI. Intracellular levels of MTI in iRBCs reached 6 μM (in infected erythrocyte) and were enhanced 3-fold to 18 μM with the addition of immucillin. In RBCs, no significant increase in MTI was detectable. Inosine levels were similar to MTI levels and followed the pattern of enhanced production due to immucillin treatment (Cassera et al., 2011). In summary, culture of iRBCs in medium containing MTA leads to detectable intracellular MTI levels.

DISCUSSION

The innate immune system relies on germline-encoded PRRs to sense pathogens with subsequent initiation of an immune response (Takeuchi and Akira, 2010). Different classes of PRR, such as Toll-like receptors, C-type lectins, and nucleotide-binding oligomerization domain (NOD)-like receptors (consisting of NOD and NLRP proteins), sense microbial structures (Brubaker et al., 2015; Dolasia et al., 2018). For the *malaria tropica*-causing pathogen *P. falciparum*, several PAMPs have been reported. For example, the heme detoxification product hemozoin and GPI anchors activate the inflammasome (Ataide et al., 2014) and TLRs (Zhu et al., 2011), respectively. In addition, nucleic acid sensors, such as TLR9, cGAS (Sharma et al., 2011; Sisquella et al., 2017; Gallego-Marin et al., 2018; Hahn et al., 2018), and AIM2 (Kalantari et al., 2014), as well as the ssRNA sensors TLR7 and TLR8 (Baccarella et al., 2013; Coch et al., 2019), sense Plasmodium DNA or RNA, respectively.

How TLR7 and TLR8 sense RNA fragmentation products and/or modified nucleosides has been intensively studied (Tanji et al., 2013, 2015; Zhang et al., 2016). RNA fragments and single nucleosides derived from GU-rich RNA through digestion by RNases, such as RNase T2 or RNase 2, bind to two distinct binding sites within each TLR and activate the corresponding receptor. During stimulation of TLR7 and TLR8 with nucleosides, transfected RNA of pathogenic origin can boost TLR activation (Coch et al., 2019). In case of TLR8, also the addition of T-rich phosphorothioate oligodeoxynucleotides (poly(dT))

Table 3. Nucleoside in iRBCs and RBCs detected by HPLC

		iRBCs (μM/erythrocyte)[a]			RBCs (μM/erythrocyte)		
		Culture conditions			Culture conditions		
	Metabolite	Control[b]	Immucillin	MTA	MTA + immucillin	Control	Immucillin	MTA	MTA + immucillin
Cell pellet[c]	inosine	ND	9.81 ± 2.22[d]	9.03 ± 4.53	53.01 ± 21.76	ND	1.83 ± 0.36	0.69 ± 0.69	1.95 ± 0.39
	MTI	ND	ND	6.47 ± 2.9	18.57 ± 7.31	ND	ND	0.75 ± 0.51	ND
	MTA	ND	ND	ND	ND	ND	ND	0.64 ± 0.60	1.53 ± 1.40
		iRBCs (μM)			RBCs (μM)				
		Culture conditions			Culture conditions				
	Metabolite	Control[b]	Immucillin	MTA	MTA + immucillin	Control	Immucillin	MTA	MTA + immucillin
Supernatant	inosine	0.98 ± 0.18	4.20 ± 0.72	1.01 ± 0.19	3.72 ± 0.79	ND	ND	ND	ND
	MTI	ND	ND	64.88 ± 11.46	67.46 ± 10.09	ND	ND	7.33 ± 1.46	0.58 ± 0.24
	MTA	ND	ND	13.87 ± 3.61	14.62 ± 3.24	ND	ND	96.16 ± 19.29	105.76 ± 17.09

ND, not detected.
[a]Number of iRBCs adjusted to parasitemia (5% or 10%).
[b]Control condition: culture medium with 100 μM hypoxanthine; for additional conditions, immucillin (10 μM) and/or MTA (100 μM) were added.
[c]Concentration in micromoles per erythrocyte (volume of 90 fL) of Miccio et al. (2015).
[d]Values indicate mean + SEM (biological replicates: 3, technical replicate: 1).

strongly enhance TLR8 sensitivity to nucleosides by an unknown mechanism (Jurk et al., 2006).

Modified natural nucleosides, such as 7-methylguanosine, 8-hydroxyguanosine (8-OHG), and 8-hydroxydeoxyguanosine (8-OHdG), activate TLR7 (Shibata et al., 2016), but for TLR8, no active natural modified nucleoside has been described. Here, we demonstrate by genetic analysis and using the hTLR8 antagonist CU-CPT9a (Hu et al., 2018; Zhang et al., 2018b) that MTI, a modified purine specific for *Plasmodium ssp.* (Ting et al., 2005; Ho et al., 2009) activates TLR8 and presumably binds to binding pocket 1 as investigated by molecular modeling and docking. Interestingly, MTI does not occur in vertebrates and is specifically part of the purine salvage pathway in Plasmodium that utilizes unique substrates to generate hypoxanthine. Accordingly, MTA, a byproduct of the polyamine metabolism, is converted to MTI by *Pf*ADA and further metabolized to hypoxanthine by *Pf*PNP. Interestingly, MTI levels (measured by mass spectrometry) naturally fluctuate in synchronized cultures of *P. falciparum* periodically (between 1- and 250-fold) during the 48 h intraerythrocytic developmental cycle, reaching its peak at 32 h post-infection (Olszewski et al., 2009). Unfortunately, the molarity of MTI per infected erythrocyte was not reported. Utilizing HPLC, we detected MTI in iRBCs at low micromolar levels (6–18 μM) when the culture medium was supplemented with MTA or MTA and immucillin. Upon ingestion of iRBCs by macrophages, endosomal MTI concentrations could reach a similar concentration, inducing IL-6 in a TLR8-dependent manner. The MTI concentrations used for *in vitro* TLR8 activation refer to 3 mM and are at least 250 times higher. Since it is unknown how efficiently extracellular-added MTI is taken up by immune cells, we speculate that only a minor fraction ends up in the endosome of monocytes, possibly reaching a concentration in the micromolar range.

We propose that MTI serves as a Plasmodium-derived PAMP for TLR8-mediated innate sensing infection. Other means of influencing MTI concentrations may be the use of immucillins, which mimic the transition states of N-ribosyltransferases and have been used to target disease-related enzymes in protozoan parasites, bacteria, and viruses (Evans et al., 2018). For example, DADMe-immucillin-H inhibits the enzyme *Pf*PNP that metabolizes MTI to hypoxanthine. Blocking this pathway leads to a block in the purine salvage pathway and to death of hypoxanthine auxotroph Plasmodium. In addition, the block should lead to accumulation of MTI with enhanced TLR8 activation. Since we have demonstrated that the addition of *P. falciparum* RNA strongly enhances MTI-driven TLR8 activation, we hypothesize that, during Plasmodium infection, optimal sensing is mediated by MTI and oligoribonucleotides derived from plasmodial RNA.

In summary, we have identified the purine MTI as a new natural human TLR8 ligand leading to proinflammatory cytokine production. The use of immucillins may boost TLR8-mediated immunity against Plasmodium by accumulation of MTI. Since MTI is also found in some pathogenic bacteria, such as *Pseudomonas aeruginosa* (Guan et al., 2011), it will be also interesting to investigate MTI-TLR8 in sensing bacterial infection.

Limitations of the study

This study identifies MTI, a *Plasmodium*-derived metabolite of the purine salvage pathway, as new TLR8 ligand. *In vitro* infection experiments with human PBMCs and *P. falciparum*-infected iRBCs suggest that MTI serves as TLR8-dependent PAMP for the production of proinflammatory cytokines, such as IL-6. It is currently not resolved whether, during a Plasmodium infection, *in vivo* MTI concentrations in the endosome would be sufficient to trigger a TLR8 response. In addition, no infection model has been studied to address the immunostimulatory role of MTI in sensing and initiating an immune response against *Plasmodium in vivo*. Since murine TLR8 does not recognize human TLR8 ligands (Hemmi et al., 2002; Lund et al., 2004), a corresponding infection model in non-human primates (Cassera et al., 2011) is essential for further addressing the role of MTI sensing in *Plasmodium* infection.

STAR★METHODS

Detailed methods are provided in the online version of this paper and include the following:

- KEY RESOURCES TABLE
- RESOURCE AVAILABILITY
  - Lead contact
  - Materials availability
  - Data and code availability
- EXPERIMENTAL MODEL AND SUBJECT DETAILS
  - Animals
  - Human subjects
  - Parasite *Plasmodium falciparum*
  - Cell lines
  - Primary cell cultures
- METHOD DETAILS
  - Reagents
  - Generation of MTI
  - RP-HPLC
  - Cell stimulation assays
  - Luciferase assay
  - TLR8 inhibitor and cell stimulation
  - ELISA
  - *P. falciparum* lysates and conversion of MTA to MTI
  - Intracellular nucleoside levels in RBC and *P. falciparum* infected RBC
  - RNA extraction
  - Phagocytosis experiments
  - TLR8-MTI docking experiments
- QUANTIFICATION AND STATISTICAL ANALYSIS

ACKNOWLEDGMENTS

We thank G. Bein, Institute for Clinical Immunology and Transfusion Medicine, Justus-Liebig-University Giessen, for providing human buffy coats. TLR8 inhibitor CU-CPT9a was kindly provided by Kerstin Mark and Prof Dr. Wibke E. Diederich, Center for Tumor Biology and Immunology, Core Facility Medicinal Chemistry, Philipps-Universität Marburg. We thank Gerhard Klebe, Institute for Pharmaceutical Chemistry, Philipps-Universität Marburg, for support on molecular modeling. We are grateful to Vern Schramm, Albert Einstein College of Medicine, New York, for providing DADMe-Immucillin-H. This work was supported by Deutsche Forschungsgemeinschaft (DFG) project 251836267, KO 4858/1-1, and Philipps-University Marburg intramural funding to G.K. and by the DFG - project ID 369799452 – TRR237 - A02 and project ID 114933180-TR84 - C10—to S. Bauer. Open Access funding provided by the Open Access Publication Funds of Philipps-Universität Marburg with support of the DFG.

AUTHOR CONTRIBUTIONS

Conceptualization, G.K., K.L., and S. Bauer; methodology, G.K., K.L., and S. Baumeister; investigation, G.K., F.V.S., H.-L.O., J.E., T.M., T.R., S.M., and S. Bauer; writing – original draft, G.K., H.-L.O., and S. Bauer; writing – review & editing, G.K., F.V.S., S. Baumeister, J.M.P., H.-L.O., and S. Bauer; funding acquisition, G.K. and S. Bauer; resources, S. Baumeister, T.V., H.H., and J.M.P.; supervision, G.K., K.L., and S. Bauer.

DECLARATION OF INTERESTS

The authors declare no competing interests.

Received: July 7, 2020
Revised: February 2, 2022
Accepted: March 25, 2022
Published: April 12, 2022

REFERENCES

Ataide, M.A., Andrade, W.A., Zamboni, D.S., Wang, D., Souza, M.d.C., Franklin, B.S., Elian, S., Martins, F.S., Pereira, D., Reed, G., et al. (2014). Malaria-induced NLRP12/NLRP3-dependent caspase-1 activation mediates inflammation and hypersensitivity to bacterial superinfection. PLoS Pathog. *10*, e1003885.

Baccarella, A., Fontana, M.F., Chen, E.C., and Kim, C.C. (2013). Toll-like receptor 7 mediates early innate immune responses to malaria. Infect. Immun. *81*, 4431–4442.

Bauernfeind, F., and Hornung, V. (2013). Of inflammasomes and pathogens–sensing of microbes by the inflammasome. EMBO Mol. Med. *5*, 814–826.

Brubaker, S.W., Bonham, K.S., Zanoni, I., and Kagan, J.C. (2015). Innate immune pattern recognition: a cell biological perspective. Annu. Rev. Immunol. *33*, 257–290.

Cassera, M.B., Hazleton, K.Z., Merino, E.F., Obaldia, N., Ho, M.-C., Murkin, A.S., DePinto, R., Gutierrez, J.A., Almo, S.C., Evans, G.B., et al. (2011). Plasmodium falciparum parasites are killed by a transition state analogue of purine nucleoside phosphorylase in a primate animal model. PLoS One *6*, e26916.

Coch, C., Hommertgen, B., Zillinger, T., Daßler-Plenker, J., Putschli, B., Nastaly, M., Kümmerer, B.M., Scheunemann, J.F., Schumak, B., Specht, S., et al. (2019). Human TLR8 senses RNA from plasmodium falciparum-infected red blood cells which is uniquely required for the IFN-γ response in NK cells. Front. Immunol. *10*, 371.

Diebold, S.S., Kaisho, T., Hemmi, H., Akira, S., and Reis e Sousa, C. (2004). Innate antiviral responses by means of TLR7-mediated recognition of single-stranded RNA. Science *303*, 1529–1531.

Dolasia, K., Bisht, M.K., Pradhan, G., Udgata, A., and Mukhopadhyay, S. (2018). TLRs/NLRs: shaping the landscape of host immunity. Int. Rev. Immunol. *37*, 3–19.

Evans, G.B., Tyler, P.C., and Schramm, V.L. (2018). Immucillins in infectious diseases. ACS Infect. Dis. *4*, 107–117.

Forsbach, A., Nemorin, J.-G., Montino, C., Müller, C., Samulowitz, U., Vicari, A.P., Jurk, M., Mutwiri, G.K., Krieg, A.M., Lipford, G.B., et al. (2008). Identification of RNA sequence motifs stimulating sequence-specific TLR8-dependent immune responses. J. Immunol. *180*, 3729–3738.

Gaidt, M.M., Rapino, F., Graf, T., and Hornung, V. (2018). Modeling primary human monocytes with the trans-differentiation cell line BLaER1. Methods Mol. Biol. *1714*, 57–66.

Gallego-Marin, C., Schrum, J.E., Andrade, W.A., Shaffer, S.A., Giraldo, L.F., Lasso, A.M., Kurt-Jones, E.A., Fitzgerald, K.A., and Golenbock, D.T. (2018). Cyclic GMP-AMP synthase is the cytosolic sensor of plasmodium falciparum genomic DNA and activates type I IFN in malaria. J. Immunol. *200*, 768–774.

Gazzinelli, R.T., Kalantari, P., Fitzgerald, K.A., and Golenbock, D.T. (2014). Innate sensing of malaria parasites. Nat. Rev. Immunol. *14*, 744–757.

Greulich, W., Wagner, M., Gaidt, M.M., Stafford, C., Cheng, Y., Linder, A., Carell, T., and Hornung, V. (2019). TLR8 Is a sensor of RNase T2 degradation products. Cell *179*, 1264–1275.e13.

Guan, R., Ho, M.-C., Almo, S.C., and Schramm, V.L. (2011). Methylthioinosine phosphorylase from Pseudomonas aeruginosa. structure and annotation of a novel enzyme in quorum sensing. Biochemistry *50*, 1247–1254.

Hahn, W.O., Butler, N.S., Lindner, S.E., Akilesh, H.M., Sather, D.N., Kappe, S.H., Hamerman, J.A., Gale, M., Liles, W.C., and Pepper, M. (2018). cGAS-mediated control of blood-stage malaria promotes Plasmodium-specific germinal center responses. JCI insight *3*, e94142.

Heil, F., Ahmad-Nejad, P., Hemmi, H., Hochrein, H., Ampenberger, F., Gellert, T., Dietrich, H., Lipford, G., Takeda, K., Akira, S., et al. (2003). The Toll-like receptor 7 (TLR7)-specific stimulus loxoribine uncovers a strong relationship within the TLR7, 8 and 9 subfamily. Eur. J. Immunol. *33*, 2987–2997.

Heil, F., Hemmi, H., Hochrein, H., Ampenberger, F., Kirschning, C., Akira, S., Lipford, G., Wagner, H., and Bauer, S. (2004). Species-specific recognition of single-stranded RNA via toll-like receptor 7 and 8. Science *303*, 1526–1529.

Hemmi, H., Kaisho, T., Takeuchi, O., Sato, S., Sanjo, H., Hoshino, K., Horiuchi, T., Tomizawa, H., Takeda, K., and Akira, S. (2002). Small anti-viral compounds activate immune cells via the TLR7 MyD88-dependent signaling pathway. Nat. Immunol. *3*, 196–200.

Hendlich, M., Rippmann, F., and Barnickel, G. (1997). LIGSITE: automatic and efficient detection of potential small molecule-binding sites in proteins. J. Mol. Graph. Model. *15*, 359-63–389.

Ho, M.-C., Cassera, M.B., Madrid, D.C., Ting, L.-M., Tyler, P.C., Kim, K., Almo, S.C., and Schramm, V.L. (2009). Structural and metabolic specificity of methylthiocoformycin for malarial adenosine deaminases. Biochemistry *48*, 9618–9626.

Hu, Z., Tanji, H., Jiang, S., Zhang, S., Koo, K., Chan, J., Sakaniwa, K., Ohto, U., Candia, A., Shimizu, T., et al. (2018). Small-Molecule TLR8 antagonists via structure-based rational design. Cell Chem. Biol. *25*, 1286–1291.e3.

Jones, G., Willett, P., Glen, R.C., Leach, A.R., and Taylor, R. (1997). Development and validation of a genetic algorithm for flexible docking. J. Mol. Biol. *267*, 727–748.

Jung, S., von Thülen, T., Laukemper, V., Pigisch, S., Hangel, D., Wagner, H., Kaufmann, A., and Bauer, S. (2015). A single naturally occurring 2'-O-methylation converts a TLR7- and TLR8-activating RNA into a TLR8-specific ligand. PLoS One *10*, e0120498.

Jurk, M., Heil, F., Vollmer, J., Schetter, C., Krieg, A.M., Wagner, H., Lipford, G., and Bauer, S. (2002). Human TLR7 or TLR8 independently confer responsiveness to the antiviral compound R-848. Nat. Immunol. *3*, 499.

Jurk, M., Kritzler, A., Schulte, B., Tluk, S., Schetter, C., Krieg, A.M., and Vollmer, J. (2006). Modulating responsiveness of human TLR7 and 8 to small molecule ligands with T-rich phosphorothiate oligodeoxynucleotides. Eur. J. Immunol. *36*, 1815–1826.

Kalantari, P. (2018). The emerging role of pattern recognition receptors in the pathogenesis of malaria. Vaccines *6*, 13.

Kalantari, P., DeOliveira, R.B., Chan, J., Corbett, Y., Rathinam, V., Stutz, A., Latz, E., Gazzinelli, R.T., Golenbock, D.T., and Fitzgerald, K.A. (2014). Dual engagement of the NLRP3 and AIM2 inflammasomes by plasmodium-derived hemozoin and DNA during malaria. Cell Rep. *6*, 196–210.

Kotra, L.P., Manouilov, K.K., Cretton-Scott, E., Sommadossi, J.P., Boudinot, F.D., Schinazi, R.F., and Chu, C.K. (1996). Synthesis, biotransformation, and pharmacokinetic studies of 9-(beta-D-arabinofuranosyl)-6-azidopurine: a prodrug for ara-A designed to utilize the azide reduction pathway. J. Med. Chem. *39*, 5202–5207.

Krüger, A., Oldenburg, M., Chebrolu, C., Beisser, D., Kolter, J., Sigmund, A.M., Steinmann, J., Schäfer, S., Hochrein, H., Rahmann, S., et al. (2015). Human TLR8 senses UR/URR motifs in bacterial and mitochondrial RNA. EMBO Rep. *16*, 1656–1663.

Lambros, C., and Vanderberg, J.P. (1979). Synchronization of Plasmodium falciparum erythrocytic stages in culture. J. Parasitol. *65*, 418–420.

Lee, J., Chuang, T.-H., Redecke, V., She, L., Pitha, P.M., Carson, D.A., Raz, E., and Cottam, H.B. (2003). Molecular basis for the immunostimulatory activity of guanine nucleoside analogs: activation of Toll-like receptor 7. Proc. Natl. Acad. Sci. U S A *100*, 6646–6651.

Lee, S.H., and Cho, Y.D. (1998). Induction of apoptosis in leukemia U937 cells by 5'-deoxy-5'-methylthioadenosine, a potent inhibitor of protein carboxylmethyltransferase. Exp. Cell Res. *240*, 282–292.

Lund, J.M., Alexopoulou, L., Sato, A., Karow, M., Adams, N.C., Gale, N.W., Iwasaki, A., and Flavell, R.A. (2004). Recognition of single-stranded RNA viruses by Toll-like receptor 7. Proc. Natl. Acad. Sci. U S A *101*, 5598–5603.

Miccio, L., Memmolo, P., Merola, F., Netti, P.A., and Ferraro, P. (2015). Red blood cell as an adaptive optofluidic microlens. Nat. Commun. *6*, 6502.

Miller, D.V., Rauch, B.J., Harich, K., Xu, H., Perona, J.J., and White, R.H. (2018). Promiscuity of methionine salvage pathway enzymes in Methanocaldococcus jannaschii. Microbiology (Reading, England) *164*, 969–981.

O'Boyle, N.M., Banck, M., James, C.A., Morley, C., Vandermeersch, T., and Hutchison, G.R. (2011). Open Babel: an open chemical toolbox. J. Cheminf. *3*, 33.

Olszewski, K.L., Morrisey, J.M., Wilinski, D., Burns, J.M., Vaidya, A.B., Rabinowitz, J.D., and Llinás, M. (2009). Host-parasite interactions revealed by Plasmodium falciparum metabolomics. Cell host & microbe *5*, 191–199.

O'Neill, L.A.J. (2006). How Toll-like receptors signal: what we know and what we don't know. Curr. Opin. Immunol. *18*, 3–9.

Ostendorf, T., Zillinger, T., Andryka, K., Schlee-Guimaraes, T.M., Schmitz, S., Marx, S., Bayrak, K., Linke, R., Salgert, S., Wegner, J., et al. (2020). Immune sensing of synthetic, bacterial, and protozoan rna by toll-like receptor 8 requires coordinated processing by RNase T2 and RNase 2. Immunity *52*, 591–605.e6.

Rapino, F., Robles, E.F., Richter-Larrea, J.A., Kallin, E.M., Martinez-Climent, J.A., and Graf, T. (2013). C/EBPα induces highly efficient macrophage transdifferentiation of B lymphoma and leukemia cell lines and impairs their tumorigenicity. Cell Rep. *3*, 1153–1163.

Rarey, M., Kramer, B., Lengauer, T., and Klebe, G. (1996). A fast flexible docking method using an incremental construction algorithm. J. Mol. Biol. *261*, 470–489.

Riscoe, M.K., Tower, P.A., and Ferro, A.J. (1984). Mechanism of action of 5'-methylthioadenosine in S49 cells. Biochem. Pharmacol. *33*, 3639–3643.

Sarvestani, S.T., Tate, M.D., Moffat, J.M., Jacobi, A.M., Behlke, M.A., Miller, A.R., Beckham, S.A., McCoy, C.E., Chen, W., Mintern, J.D., et al. (2014). Inosine-mediated modulation of RNA sensing by Toll-like receptor 7 (TLR7) and TLR8. J. Virol. *88*, 799–810.

Schneider, N., Lange, G., Hindle, S., Klein, R., and Rarey, M. (2013). A consistent description of HYdrogen bond and DEhydration energies in protein-ligand complexes: methods behind the HYDE scoring function. J. Comput. Aided Mol. Des. *27*, 15–29.

Sharma, S., DeOliveira, R.B., Kalantari, P., Parroche, P., Goutagny, N., Jiang, Z., Chan, J., Bartholomeu, D.C., Lauw, F., Hall, J.P., et al. (2011). Innate immune recognition of an AT-rich stem-loop DNA motif in the Plasmodium falciparum genome. Immunity *35*, 194–207.

Shibata, T., Ohto, U., Nomura, S., Kibata, K., Motoi, Y., Zhang, Y., Murakami, Y., Fukui, R., Ishimoto, T., Sano, S., et al. (2016). Guanosine and its modified derivatives are endogenous ligands for TLR7. Int. Immunol. *28*, 211–222.

Sisquella, X., Ofir-Birin, Y., Pimentel, M.A., Cheng, L., Abou Karam, P., Sampaio, N.G., Penington, J.S., Connolly, D., Giladi, T., Scicluna, B.J., et al. (2017). Malaria parasite DNA-harbouring vesicles activate cytosolic immune sensors. Nat. Commun. *8*, 1985.

Takeuchi, O., and Akira, S. (2010). Pattern recognition receptors and inflammation. Cell *140*, 805–820.

Tanji, H., Ohto, U., Shibata, T., Miyake, K., and Shimizu, T. (2013). Structural reorganization of the Toll-like receptor 8 dimer induced by agonistic ligands. Science (New York, N.Y.) *339*, 1426–1429.

Tanji, H., Ohto, U., Shibata, T., Taoka, M., Yamauchi, Y., Isobe, T., Miyake, K., and Shimizu, T. (2015). Toll-like receptor 8 senses degradation products of single-stranded RNA. Nat. Struct. Mol. Biol. *22*, 109–115.

Ting, L.-M., Shi, W., Lewandowicz, A., Singh, V., Mwakingwe, A., Birck, M.R., Ringia, E.A.T., Bench, G., Madrid, D.C., Tyler, P.C., et al. (2005). Targeting a novel Plasmodium falciparum purine recycling pathway with specific immucillins. J. Biol. Chem. *280*, 9547–9554.

Trager, W., and Jensen, J.B. (1976). Human malaria parasites in continuous culture. Science *193*, 673–675.

Venegas, F.A., Köllisch, G., Mark, K., Diederich, W.E., Kaufmann, A., Bauer, S., Chavarría, M., Araya, J.J., and García-Piñeres, A.J. (2019). The bacterial product violacein exerts an immunostimulatory effect via TLR8. Sci. Rep. *9*, 13661.

Vierbuchen, T., Bang, C., Rosigkeit, H., Schmitz, R.A., and Heine, H. (2017). The human-associated archaeon methanosphaera stadtmanae is recognized through its RNA and induces TLR8-dependent NLRP3 inflammasome activation. Front. Immunol. *8*, 1535.

Webster, H.K., Wiesmann, W.P., and Pavia, C.S. (1984). Adenosine deaminase in malaria infection: effect of 2'-deoxycoformycin in vivo. Adv. Exp. Med. Biol. *165 Pt A*, 225–229.

Zhang, S., Hu, Z., Tanji, H., Jiang, S., Das, N., Li, J., Sakaniwa, K., Jin, J., Bian, Y., Ohto, U., et al. (2018a). Small-molecule inhibition of TLR8 through stabilization of its resting state. Nat. Chem. Biol. *14*, 58–64.

Zhang, Z., Ohto, U., Shibata, T., Krayukhina, E., Taoka, M., Yamauchi, Y., Tanji, H., Isobe, T., Uchiyama, S., Miyake, K., et al. (2016). Structural analysis reveals that toll-like receptor 7 is a dual receptor for guanosine and single-stranded RNA. Immunity *45*, 737–748.

Zhang, Z., Ohto, U., Shibata, T., Taoka, M., Yamauchi, Y., Sato, R., Shukla, N.M., David, S.A., Isobe, T., Miyake, K., et al. (2018b). Structural analyses of toll-like receptor 7 reveal detailed RNA sequence specificity and recognition mechanism of agonistic ligands. Cell Rep. *25*, 3371–3381.e5.

Zhu, J., Krishnegowda, G., Li, G., and Gowda, D.C. (2011). Proinflammatory responses by glycosylphosphatidylinositols (GPIs) of Plasmodium falciparum are mainly mediated through the recognition of TLR2/TLR1. Exp. Parasitol. *128*, 205–211.

STAR★METHODS

KEY RESOURCES TABLE

REAGENT or RESOURCE	SOURCE	IDENTIFIER
Antibodies		
Rat anti-human IL-6, clone MQ2-13A5	BD Pharmingen	Cat# 554543; RRID:AB_398568
Rat anti-human IL-6 biotinylated, clone MQ2-39C3	BD Pharmingen	Cat# 554546; RRID:AB_395470
Mouse anti-human IL-1β, clone 2805	R&D	Cat# MAB601; RRID:AB_358545
Goat anti-human IL-1β biotinylated	R&D	Cat# BAF201; RRID:AB_356214
Anti-mouse IL-6	R&D	Cat# MAB406; RRID:AB_2233899
Rat anti-mouse IL-6 biotinylated	R&D	Cat# BAF406; RRID:AB_356455
Anti-human TNF-α	BD Pharmingen	Cat # 551220; RRID:AB_394098
Anti-human TNF-α biotinylated	BD Pharmingen	Cat # 554511; RRID:AB_395442
Mouse anti-human CD14-APC	BioLegend	Cat# 301807; RRID:AB_314189
Mouse-anti-human CD19-PE	BioLegend	Cat# 302254; RRID:AB_2564142
Biological samples		
Buffy coats for isolation of PBMCs and monocytes	Hackstein and G. Bein, Institute for Clinical Immunology and Transfusion Medicine, Justus-Liebig-University Giessen	N/A
Chemicals, peptides, and recombinant proteins		
Streptavidin-POD	Roche	Cat# 11089153001
Pam3Cys	InvivoGen	Cat# tlrl-pms
Resiquimod (R848)	InvivoGen	Cat# tlrl-r848
TL8-506	InvivoGen	Cat# tlrl-tl8506
Lipopolysaccharid from *Escherichia coli* 0111:B4	InvivoGen	Cat# tlrl-eblps
Lipoprotein-Lipase aus Pseudomonas sp.	Sigma-Aldrich	Cat# L9656
Poly(dT)	InvivoGen	Cat# tlrl-pt17
Methylthioadenosin (5′-MTA)	Calbiochem	Cat# 260585
Methylthioinosine (5′-MTI)	this manuscript	N/A
Human IL-1β	PeproTech	Cat# 200-01B-2UG
Human IL-6	ImmunoTools	Cat# 11340064
Murine IL-6	R&D	Cat# 406-ML
Human IL-3	PeproTech	Cat# 200-03
Human TNF-α	PeproTech	Cat# 300-01A
Human M-CSF	PeproTech	Cat# 300-25
DADMe-Immucillin-H	Vern Schramm, New York	N/A
Pentostatin	Sigma-Aldrich	Cat# SML0508
Adenosine	Sigma-Aldrich	Cat# A-4036
Inosine	Sigma-Aldrich	Cat# I-4125
β-estradiol	Sigma-Aldrich	Cat# E2758
Hypoxanthine	C.C Pro GmbH	Cat# Z-41-M
Gentamicin-sulfate	Sigma-Aldrich	Cat# G1914
Human erythrocytes and serum from A+ or 0 + donors	Reagents were purchased from Blood Bank Universitätsklinikum Giessen and Marburg GmbH (UKGM), Germany	N/A
QUANTI-Blue™ Solution	InvivoGen	Cat# rep-qb1
Poly L-Arginine hydrochloride	Sigma-Aldrich	Cat# P7762
Coelenterazin	PJK	Cat# 102171
2xGaussia Lysis Buffer	PJK	Cat# 102517

(*Continued on next page*)

Continued

REAGENT or RESOURCE	SOURCE	IDENTIFIER
Human serum defibrinated, AB	Sigma-Aldrich	Cat# H4522
recombinant murine GM-CSF	PeproTech	Cat# 315-02
Anti-malaria (Plasmodium falciparum) human serum	NIBSC	Product number: 10/198
DOTAP	Roche	Cat# 11202375001
RPMI 1640	Gibco	Cat# 52400-041
DMEM	Life Technologies	Cat# 11960-085
Pancoll	PAN-Biotech	Cat# P04-60500
Percoll	Sigma-Aldrich	Cat# GE17-0891-02
Trizol	Thermofisher	Cat# 15596026
Zeocin	InvivoGen	Cat# ant-zn-1
Blasticidin	InvivoGen	Cat# ant-bl-5b
Normocin	InvivoGen	Cat# ant-nr-1
RNeasy Mini Kit	Qiagen	Cat# 74104
Fetal calf serum (FCS)	Sigma	Cat# F7524
Flt3-L	Supernatant produced within Department for Immunology	N/A
CuCPT9a	Synthesized by Wibke Diederich, University of Marburg	N/A
L-Glutamine	PAN Biotech	Cat# P04-80100
Penicillin-Streptomycin	PAN Biotech	Cat# P06-07100
MEM non-essential amino acids solution (100x)	Gibco	Cat# 11,140-035
OptiMem	Gibco	Cat# 31,985-047
2-mercaptoethanol	Gibco	Cat# 31,350-010
Neomycin solution	Sigma-Aldrich	Cat# N1142
Formic acid	Roth	Cat# 4724.3
Sodium nitrite	Sigma-Aldrich	Cat# S2252
Acetonitrile	Roth	Cat# 8825.2
Ammonium acetate	Roth	Cat# 7869.1
Saponine	Sigma-Aldrich	Cat# 47036
D-Sorbit	Carl Roth	Cat# 6213.1
Sodium acetate	Sigma-Aldrich	Cat# S2889
Acetic acid	Roth	Cat# 3738.1
Sodium pyruvate	PAN-Biotech	Cat# P04-43100
Critical commercial assays		
Universal Mycoplasma Detection Kit	ATCC	Cat# 30-1012K
Experimental models: Cell lines		
HEK 293 TLR7+	Thomas Zillinger, Bonn	N/A
HEK 293 TLR8+	Thomas Zillinger, Bonn	N/A
HEK 293 TLR7+ NF-κB+	this manuscript	N/A
HEK 293 TLR8+ NF-κB+	this manuscript	N/A
THP1 cells	Carsten Kirschning, Essen	RRID:CVCL_0006
BLaER1 cells	Holger Heine, Borstel	RRID:CVCL_VQ57
HEK Blue cells TLR8+	InvivoGen	Cat# kb-htlr8
Experimental models: Organisms/strains		
WT C57BL/6	Harlan, Envigo	N/A
Plasmodium falciparum strain 3D7	Klaus Lingelbach, Marburg	N/A

(*Continued on next page*)

Continued

REAGENT or RESOURCE	SOURCE	IDENTIFIER
Oligonucleotides		
Poly(I:C) (HMW)	InvivoGen	Cat# tlrl-pic
ORN06S (5′-UsUsGsUsUsGsUsUsGsUsUsGsUsUs GsUsUsGsUsU-3′); "s" depicts phosphorothioate linkage	MWG Eurofins	N/A
pGL3-Gluc	Thomas Zillinger, University of Bonn	N/A
pMSCVpuro	Institute for Immunology, University of Marburg	N/A
Sep-Pak Column C18	Waters	Cat# WATEWAT020515
Supelco Discovery BIO Wide Pore C18 column (250 × 10 mm, 10μm)	Sigma-Aldrich	Cat# 568223-U
CS Column	Miltenyi Biotech	1 Cat# 30-041-305
Supelcosil LC-18-S column (250 × 4.6 mm, 5μm)	Sigma-Aldrich	Cat# 58928-U
Software and algorithms		
SoftMaxPro Elisa Software V 5.0.1	Molecular Devices	N/A
Graph Pad Prism 8.4.2		N/A

RESOURCE AVAILABILITY

Lead contact

Further information and requests for resources and reagents should be directed to and will be fulfilled by the Lead Contact, Stefan Bauer (stefan.bauer@staff.uni-marburg.de).

Materials availability

This study did not generate new unique reagents.

Data and code availability

- Original/source data for all figures in the paper are available from the lead contact upon request
- This paper does not report original code.
- Any additional information required to reanalyze the data reported in this paper is available from the lead contact upon request.

EXPERIMENTAL MODEL AND SUBJECT DETAILS

Animals

Female or male C57BL/6 mice were obtained from Harlan, Envigo, Germany and used at an age between 8 and 12 weeks for the generation of murine immune cells from mouse bone marrow. These experiments were performed in accordance with the National German welfare law §4 (3) TierSchG and §2 and Annex 2 (TierSchVerV) of the National Order for the use of animals in research and did not need the approval by a local ethics committee. According to the regulations, the number of mice used was reported to the animal welfare officer of the Philipps-University Marburg.

Human subjects

Human peripheral blood mononuclear cells (hPBMC) were isolated by Pancoll (PAN Biotech) density centrifugation from whole blood (buffy coats) donated by anonymous healthy volunteers. Informed consent was obtained from all blood donors. The local ethics committees of Justus-Liebig-University Gießen and Philipps-University Marburg approved the use of human blood samples for this study. Monocytes were enriched from freshly isolated hPBMC using Percoll (Sigma-Aldrich).

Parasite *Plasmodium falciparum*

Plasmodium falciparum strain 3D7 was grown and maintained in continuous culture as described previously (Trager and Jensen, 1976). Parasites were grown at 37°C, 5% (v/v) CO_2 and 5% (v/v) O_2 in RPMI 1640 growth medium supplemented with 10% heat inactivated plasma (human, type A+), 200 mM hypoxanthine (C.C Pro GmbH, Oberdorla, Germany) and 20 mg/mL gentamicin (Sigma-Aldrich) at a hematocrit of 4% (v/v) of human erythrocytes (type A+ or O+ in phagocytosis experiments). Human red blood cells (RBC) and human serum were purchased from Blood Bank Universitätsklinikum Giessen and Marburg GmbH (UKGM), Germany. For experiments presented in Figure 5 and Table 2, parasites were grown at 8% (v/v) CO_2 without the standard gas mixture. Similar parasite

growth and reproduction characteristics were observed when compared to standard culture conditions. Synchronization of cultures to ring stage was achieved by using sorbitol (Carl Roth, Arlesheim, Switzerland) (Lambros and Vanderberg, 1979). Parasite cultures were routinely checked for mycoplasma contamination with a PCR mycoplasma test kit (ATCC, Manassas, US) or with a reporter HEK-293T cell line expressingTLR2-and a NF-κB luciferase (kind gift of Markus Schnare, Philipps University Marburg).

Cell lines

Human embryonic kidney cells (HEK-293T) stably transfected with human TLR8 (293xl-htlr8) or human TLR7 (293xl-htlr7) were obtained from InvivoGen (Toulouse, France) and cultivated in Dulbecco's modified Eagle's medium (Life Technologies, Darmstadt, Germany) supplemented with 10% FCS (Gibco), 2 mM L-glutamine, 100 U/mL penicillin G and 100 μg/mL streptomycin sulphate (PAN Biotech, Aidenbach, Germany), 0.1% 2-mercaptoethanol (Gibco). Both cell lines were stably transfected with the NF-kB reporter plasmid (pGL3-Gluc, Thomas Zillinger, University of Bonn, Germany) by co-transfection with the plasmid pMSCVpuro (conferring Puromycin resistance). After selection and clonal expansion, these reporter cells named HEK TLR7+Nf+ or HEK TLR8+Nf+ were used for stimulation. For some experiments HEK-blue hTLR8 (InvivoGen, Toulouse, France, #hkb-htlr8) were analyzed. Cells were cultured in DMEM medium supplemented with 10% heat-inactivated FCS, 1% penicillin and streptomycin, 100 μg/mL normocin (InvivoGen), 30 μg/mL blasticidin (InvivoGen) and 100 μg/mL zeocin (InvivoGen) in a 5% CO2 humidified atmosphere at 37°C.

The B-cell line BLaER1 (Rapino et al., 2013) and the CRISPR/Cas9 generated knock-outs BLaER1 TLR7ko and BLaER1 TLR8ko (Vierbuchen et al., 2017) were cultured in RPMI 1640 medium (PAN Biotech) supplemented with 10% FCS, 2 mM L-glutamine, 100 U/mL penicillin G, 100 μg/mL streptomycin sulphate and 1 mM sodium pyruvate (PAN-Biotech) at a cell density between 1×10^5 and 2×10^6 cells/mL. Transdifferentiation from B-cells to monocytes was induced by cultivating 3×10^5 cells/mL for 6–7 days in complete medium with 10 ng/mL IL-3, 10 ng/mL M-CSF (both PeproTech), and 100 nM β–estradiol (Sigma-Aldrich) (Rapino et al., 2013; Vierbuchen et al., 2017). Transdifferentiated BLaER1 cells were plated in complete medium without IL-3, M-CSF, or β-estradiol and the identity of the cells was regularly checked with anti-CD19 and anti-CD14 fluorescent-labelled antibodies and subsequent flow cytometry on a FACS Calibur (BD Bioscience, Heidelberg, Germany).

THP-1 cells (kind gift of Carsten Kirschning (Essen, Germany) were cultivated in RPMI medium supplemented with 2 mM L-glutamine, 100 U/mL penicillin, 100 μg/mL streptomycin, 1 x amino acids and 10% FCS.

Primary cell cultures

Mouse bone marrow cells were cultured in OptiMEM medium (Gibco, Karlsruhe, Germany) supplemented with 100 U/mL penicillin, 100 μg/mL streptomycin, 1% FCS, 0.1% 2-mercaptoethanol and the Flt3L-supernatant at a 1:250 dilution. After 8d of culture highly enriched differentiated plasmacytoid dendritic cells (Flt3L-DC) were obtained. To generate mouse myeloid dendritic cells (mDC), bone marrow cells were cultured in RPMI supplemented with 2 mM L-glutamine, 100 U/mL penicillin, 100 μg/mL streptomycin, 0.5% 2-mercaptoethanol, 10% FCS and 10% GM-CSF containing cell culture supernatant. GM-CSF containing medium was added on day three and day six and cells were used for stimulation experiments on day seven. Mouse macrophages were differentiated out of bone marrow cells by culturing with RPMI supplemented with 2 mM L-glutamine, 100 U/mL penicillin, 100 μg/mL streptomycin, 0.1% 2-mercaptoethanol, 10% FCS and the addition of the differentiation factor M-CSF (PreproTech) at a final concentration of 20 ng/mL. On day three, M-CSF 20 ng/mL was again added to the cells. On day five, the differentiated macrophages were ready to use for experiments.

Human PBMC and monocytes were cultivated and seeded at 3×10^5 cells/well for cytokine induction in RPMI medium supplemented with 2 mM L-glutamine, 100 U/mL penicillin, 100 μg/mL streptomycin, 1 x amino acids 1mM sodium pyruvate (PAN Biotech), 2% human AB serum (Biochrom AG, Berlin, Germany).

METHOD DETAILS

Reagents

R848, TL8-506, Pam3Cys (P3Cys), poly (I:C), LPS and poly(dT) were obtained from InvivoGen (Toulouse, France). ORN06S (5′-sUsUsGsUsUsGsUsUsGsUsUsGsUsUsGsUsUsGsUsU-3′) (Forsbach et al., 2008; Tanji et al., 2015) was synthesized by MWG Eurofins (Ebersberg, Germany). Phosphorothioate protected positions of DNA ODNs are indicated by 's'. Recombinant Human Interleukin-1 beta (rh IL-1beta/IL1F2) was obtained from PeproTech (Hamburg, Germany). 5′-DADMe-Immucillin-H was a kind gift of Vern Schramm, New York, pentostatin was purchased from Sigma-Aldrich (Taufkirchen, Germany). Inosine and adenosine were from Sigma-Aldrich and MTA from Calbiochem (Darmstadt, Germany). CU-CPT9a was synthesized in the Core Facility Medicinal Chemistry, Philipps University Marburg as described (Hu et al., 2018; Zhang et al., 2018a; Venegas et al., 2019).

Generation of MTI

As MTI is not available commercially, it was produced from the nucleoside 5′-methylthioadenosine (MTA) (Calbiochem, Darmstadt, Germany) by a synthetic deamination reaction. For control experiments, adenosine (Sigma-Aldrich) was converted to inosine. MTA or adenosine were converted to MTI or inosine 100 mg MTA or adenosine were dissolved in 1.6 mL H_2O and incubated with 0.226 g sodium acetate, 500 μL acetic acid and 1 mL 60% $NaNO_2$ for 5 h (Kotra et al., 1996). After stopping the reaction, the samples were purified via Sep-Pak column (Waters, Eschborn, Germany), eluted with 40% ethanol and purified by RP-HPLC. For identification

of MTI, HR-ESI mass spectra were acquired with a LTQ-FT Ultra mass spectrometer (ThermoFischer Scientific). The resolution was set to 100.000.

RP-HPLC

Two different RP-HPLC systems were used throughout this study. For the purification of the converted MTI, RP-HPLC analysis was performed on a Dionex Ultimate 3000 System (Germering, Germany) using a Supelco Discovery BIO Wide Pore C18 column (250 × 10 mm, 10 μm) in preparative runs or a Supelcosil LC-18-S column (250 × 4.6 mm, 5 μm) in analytical runs, protected with a C18 guard column (4 × 2 mm). All columns were obtained from Sigma-Aldrich.

The mobile phase consisted of 0.1% formic acid in water (eluent A) and 40% acetonitrile (eluent B). The separation started with 100% eluent A to 36% eluent B at 14 min and a flow rate of 5 mL/min for preparative and 1.5 mL/min for analytical runs. The eluted nucleosides were recorded by UV spectrometry at 254 nm. In preparative runs, MTI or inosine fractions were collected manually and afterwards lyophilized. To check the conversion from MTA to MTI by *P. falciparum* lysates, the analysis was performed on the same Dionex Ultimate 3000 System and Sulpelcosil LC-18-S column (250 × 4,6 mm, 5 μm), but with a different buffer (NH_4Ac as additive instead of formic acid) and a different gradient and run length, as described in Jung et al., (2015). A set of different standard nucleosides (all purchased from Sigma) were used to identify the nucleoside peaks.

Cell stimulation assays

Unless otherwise stated, control stimuli were used in the following concentrations: Pam3Cys (P3Cys) 10 μg/mL, LPS 100 ng/mL, R848 0.5 μg/mL, poly(dT) 3 μM. Cell culture medium served as negative control in all experiments. Human PBMC and monocytes were seeded in 96-well plates at 3 × 10^5 cells/well, BLaER1 cells at 5 × 10^4 cells/well, mouse Flt3LDC at 2 × 10^5 cells/well, mDC and macrophages at 1.5 × 10^5 cells/well and incubated with different stimuli in 100 μL/well for 24 h before cell supernatants were subjected to ELISA. Stably transfected HEK-293 TLR8+Nf+ or TLR7+Nf+ cells were seeded at 3 × 10^4 cells/well on day 0, stimulated with the different stimuli in 100 μL/well on day 1 and lysed for luciferase assay on day 2.

When ORN06S or *Pf*RNA was used as co-stimulus, DOTAP (Roche, Penzberg, Germany or Roth, Karlsruhe, Germany) or poly L-arginine (Sigma-Aldrich) complexation was necessary. DOTAP: for one well, 25 μL of ORN06S in OptiMEM medium and 1.5 μL (PBMC and monocytes) or 3 μL (HEK-293) DOTAP in 25 μL OptiMEM were combined and incubated for 15 min 50 μL of complete medium (depending on the cell type) was then added and the final volume of 100 μL/well was used for the stimulation.

Poly L-arginine (pLA): ORN or RNA in the indicated concentration was added to 7.5 μL of PBS and 0.2 μL pLA (1 μg/mL) per well. After incubation for 10 min at RT, the volume was adjusted to 100 μL and used for stimulation experiments.

Luciferase assay

HEK-293 TLR7+Nf+ and TLR8+Nf+ cells were used for stimulation experiments and luciferase assays. After 24 h of stimulation, the supernatant was collected and discarded. 50 μL of Lysis Juice (PJK, Kleinblittersdorf, Germany) was added to each well and cells were lysed by freezing at −80°C for at least 20 min 10 μL of the lysate was mixed with 30 μL of Gaussia luciferase buffer (1.43 μM coelenterazin (PJK), 2.2 mM Na_2EDTA, 0.22 M K_3PO_4, 0.44 mg/mL BSA, 1.1 M NaCl, 1.3 mM NaN_3) and measured with a luminometer. The n-fold induction was obtained by dividing the value of the stimulus by the medium control.

TLR8 inhibitor and cell stimulation

HEK-blue hTLR8 cells were cultured in DMEM medium supplemented with 10% heat-inactivated FCS, 1% penicillin and streptomycin, 100 μg/mL normocin (InvivoGen), 30 μg/mL blasticidin (InvivoGen) and 100 μg/mL zeocin (InvivoGen) in a 5% CO_2 humidified atmosphere at 37°C. Inhibition of MTI activity by CU-CPT9a in HEK-blue hTLR8 cells. HEK-blue hTLR8 cells were seeded with a density of 4 × 10^5 live cells/mL on a 96-well plate and incubated for 24 h at 37°C, 5% CO_2. Cells were treated with different concentrations of CU-CPT9a (0, 0.1, 1 and 10 μM) along with different stimulators such as MTI (0.5 mg/mL) with poly(dT) (1 μM), R848 (1 μM) with poly(dT) (1 μM) or IL-1β (10 ng/mL) with poly(dT) (1 μM) and the plate was incubated for 16-17 h at 37°C, 5% CO_2. Subsequently, 20 μL of cultured medium of every condition was added to 180 μL of Quanti-Blue (InvivoGen) and mixed in a new 96-well plate and incubated for 1 h at 37°C, 5% CO_2. The plates were then quantified in a microplate reader (LEDETECT 96, Biomed Dr. Weiser GmbH, Salzburg, Austria) by measurement at 650 nm.

ELISA

Concentrations of murine IL-6 (R&D Wiesbaden, Germany) and human IL-6 (BD Pharmingen), human TNF-α (BD Pharmingen) and human IL-1β (R&D) in the culture supernatants were determined by ELISA according to the manufacturer's instructions.

P. falciparum lysates and conversion of MTA to MTI

A 500 μL cell pellet of iRBC (trophozoites, 10% parasitemia) and RBC was diluted with 700 μL of PBS and subjected to three freeze-thaw cycles. 50 μL of this lysate was diluted in 1 mL RPMI medium and varying amounts of MTA or adenosine together with the *Pf*PNP inhibitor DADMe-Immucillin-H or the *Pf*ADA inhibitor pentostatin were added. After 24 h at 37°C, the solution was denatured at 75°C for 20 min to delete enzyme activity and centrifuged. The supernatant was analyzed by RP-HPLC (see above) to check, if the conversion from MTA or adenosine was successful and then used in cell stimulation assays.

Intracellular nucleoside levels in RBC and *P. falciparum* infected RBC

1 or 2 × 10^9 RBC or synchronized iRBC (trophozoites, 5 or 10% parasitemia) in 5mL culture medium containing 100μM hypoxanthine were incubated with MTA (100μM) and/or immucillin (10μM) for 1h at 37°C. Cells were pelleted and 1mL supernatant centrifuged with Amicon centricon YM-10 (Millipore). iRBC or RBCs were washed 3 times in ice-cold PBS and nucleosides extracted with 5 times the pellet volume of 1M perchloric acid. After centrifugation, the soluble fraction was neutralized with 10% ammonium hydroxide solution and partially concentrated by vacuum (speedvac). For one experiment, NaCl was added to 2M and the nucleosides purified with waters Sep-Pak Plus C18 cartridges. Briefly, solution was applied to a MeOH –activated and H_2O-washed column. Thereafter, column was washed with 1.4 mL H_2O and nucleosides were eluted with 2 mL of MeOH/H2O (60:40 v/v) followed by evaporation (residual volume 160μL). In general, 100μL solutions were analyzed by HPLC (see below).

RNA extraction

P. falciparum 3D7 cultures were subjected to saponin lysis (0.1% in PBS for 10 min) to release the parasites from the red blood cells. The parasite RNA and THP-1 RNA was extracted with Trizol (Thermofisher) and an additional RNA cleanup with the RNeasy mini kit and DNase digest (Qiagen, Venlo, Netherlands) was performed. The quality of the purified RNA was checked on an agarose gel.

Phagocytosis experiments

3D7 *P. falciparum* trophozoite infected red blood cells were enriched to 95–99% parasitemia on CS- or LD columns (Miltenyi Biotech, Bergisch-Gladbach, Germany) in a magnetic VarioMACS or MidiMACS separator. In one set of experiments (Figure 4C) enriched iRBC were opsonized in anti-malaria serum (NIBSC, South Mimms, UK) at a ratio of 1:2 (1 μL packed iRBC: 2 μL anti-malaria serum) for 1 h at 37°C. After a final washing step, iRBC were ready for use in the phagocytosis assay. Human PBMC were seeded in a 96-well plate at a density of 3 × 10^5 cells/well in PBMC medium without serum and the opsonized iRBC or RBC were added at a ratio of 10:1 iRBC/PBMC. MTI was substituted to the appropriate wells in different concentrations. After 24 h, the supernatants were collected and subjected to ELISA. In another set of experiments (Figure 5) enriched parasites were opsonized with 2 μg/mL anti-D (Rh) immunoglobulin (Rhophlac 300, CSL Behring) and incubated with PMBCs adjusted to 100.000 monocytes/well at a ratio of 3:1 iRBC or RBC per monocytes in RPMI containing 2% AB serum, 20 μM hypoxanthine and in some conditions also 100 μM MTA and/or 10 μM immucillin. The TLR8 inhibitor CU-CPT9a was used at 2 μM and incubated with PBMC at 37°C 30 min prior to incubation with RBC or iRBC.

TLR8-MTI docking experiments

The LIGSITE algorithm (Hendlich et al., 1997) was applied to detect depressions on the surface of the target protein, large enough to be a putative binding site. In case of TLR8, nine possible binding sites were detected (see Table 3).

To identify the energetically most preferred binding site of 5-methylthioinosine, the following cross-docking approach was applied: Every ligand was docked into each of the nine putative binding sites of TLR8. A spatial structure for the ligands was generated with the program Open Babel (O'Boyle et al., 2011), and they were subsequently minimized with the MMFF94 forcefield. The docking was carried out with the docking program GOLD (Jones et al., 1997). In addition, another docking run was performed with the program FlexX (Rarey et al., 1996) and a rescoring of the docking solutions was accomplished with the scoring function HYDE (Schneider et al., 2013).

QUANTIFICATION AND STATISTICAL ANALYSIS

Statistical significance was analysed using one-way or two-way ANOVA followed by post hoc tests as indicated to correct for multiple comparisons. Data calculations were performed using Graph Pad Prism 8.4.1 software. Bars show mean + SEM of biological replicates. The values of $p < 0.5$ were considered to be statistically significant (*$p < 0.05$, **$p < 0.01$, ***$p < 0.001$, ****$p < 0.0001$).